EFDA–JET–CP(13)03/05

F.A. Calderon, R.O. Dendy, S.C. Chapman, A.J. Webster, B. Alper, R.M. Nicol
and JET EFDA contributors

Low Dimensional Dynamics in Type I ELMing in JET Plasmas

Low Dimensional Dynamics in Type I ELMing in JET Plasmas

F.A. Calderon[1], R.O. Dendy[2,1], S.C. Chapman[1,3], A.J. Webster[2], B. Alper[2], R.M. Nicol[1] and JET EFDA contributors*

JET-EFDA, Culham Science Centre, OX14 3DB, Abingdon, UK

[1]Centre for Fusion, Space and Astrophysics, Department of Physics, Warwick University, Coventry CV4 7AL, UK
[2]EURATOM-CCFE Fusion Association, Culham Science Centre, OX14 3DB, Abingdon, OXON, UK
[3]Department of Mathematics and Statistics, Tromsoe University, Norway
[4]JET-EFDA, Culham Science Centre, OX14 3DB, Abingdon, OXON, UK
** See annex of F. Romanelli et al, "Overview of JET Results", (24th IAEA Fusion Energy Conference, San Diego, USA (2012)).*

Preprint of Paper to be submitted for publication in Proceedings of the 40th EPS Conference on Plasma Physics, Espoo, Finland.
1st July 2013 – 5th July 2013

1. INTRODUCTION

Enhanced confinement regimes (H-mode) in tokamak plasmas are accompanied by pulses of energy and particle release known as edge localised modes (ELMs). The characteristics of ELMs, and their control, are central topics for ITER [1-3]. Theories exist for some elements of the ELMing process, but there is no first principles model incorporating all the relevant physical effects. ELM categorisation is phenomenological, and few papers [4-7] have addressed ELM sequences as the pulsed outputs of a nonlinear system. Characterisation of ELMing processes by applying dynamical systems theory to the data, as here, strengthens the scientific basis for understanding, prediction, and control. We construct [7] delay plots for the measured time intervals between successive ELMs in six similar plasmas in the JET tokamak. This set includes JET Pulse No: 57865, where the H-mode closely approaches an ITER operating regime with respect to some key dimensionless parameters. We find [7] that type I ELMing in these plasmas exhibits transitions dependent on the gas puffing rate as control parameter. In all six JET plasmas, the toroidal magnetic field density is 2.7T, the plasma current is 2.5MA, neutral beam and ion cyclotron resonance heating power are 13.5MW and 2.0MW respectively, and the H98 confinement factor is 0.87–1.0. Gas puffing terminates at 23.3s and neutral beam heating is ramped down from 23.5 to 24.5s. The differences in type I ELM character are largely determined by the different levels of externally applied gas puffing. The intensity of the D_α signal, which sometimes saturates, is not necessarily a proxy for the magnitude of the underlying ELM plasma phenomenon. However occurrence times, and hence inter-ELM time intervals, are well defined. The occurrence time of each ELM is inferred from the D_α datasets using an algorithm similar to Ref.[5], which exploits the steep leading edge of each ELM. This generates a sequence of event times tn for each nth ELM, and hence inter-event times $\delta t_n = t_n - t_{n-1}$. These sequences are used to construct delay plots, which capture key aspects[7] of the phase space evolution of the plasma physics system responsible for ELMing.

2. RESULTS

Figures 1 and 2, from Ref [7], show measured type I ELM signals for the sequence of six JET H-mode plasmas 578mn, where mn is 72, 71, 70, 65, 67, and 69 in order of increasing magnitude and duration of the gas puffing rate, shown in Fig.3. The upper trace in each panel of Figs.1 and 2 plots the time-evolving intensity of the D_α signal measured by a camera directed at the inner divertor, normalised by the mean measured intensity. The two groupings of three plasmas are at lower (Fig.1) and higher (Fig.2) gas puffing rates. In Fig.1 the ELM signal intensity is roughly the same across each time series, whereas in Fig.2 there is rich structure. We sort the ELM events that are used to construct the time series of inter-ELM time intervals, in terms of whether they exceed a threshold in signal intensity; the thresholds used are indicated by horizontal lines on the ELM time series (top panel in Figs.1 and 2). Each nth type I ELM that has signal intensity exceeding a given threshold defines an event time tn. Delay plots have axes δt_n and δt_{n+1}, where $\delta t_n = t_n - t_{n-1}$. The middle panels of Figs.1 and 2 show the delay plots for a given threshold, and the D_α signal

intensity for the ELM at tn is indicated by colour coding.

The number of ELMs evaluated in these plasmas ranges between 79 and 197. The mean inter-ELM time interval is in the range 25–60ms. The delay plots in Fig.1 are insensitive to the threshold, in contrast to Fig.2, suggesting that these reflect distinct processes. In Fig.1, plasmas with successively greater gas puffing rates are shown from left to right. Increased gas puffing causes the ELMing process to bifurcate from singly periodic (Pulse No: 57872), via transitional behaviour (Pulse No: 57871), to a situation where two periods are present (Pulse No: 57870) together, with the plasma switching between them. It is apparent that a longer delay time δtn before an ELM correlates statistically with a larger D_α signal intensity. The bottom pair of plots in each panel of Figs.1 and 2 displays the probability density functions for the distributions of measured δt_n for the ELM time series using the same amplitude thresholds as for the delay plots. In Fig.1, unlike Fig.2, these two panels are identical. Figure 2, which corresponds to higher levels of gas puffing rate, displays a transition in the ELMing process as the gas puffing rate is increased, which is different to that in Fig.1. Each ELM with large D_α signal intensity is statistically likely to be rapidly followed by a population of postcursor ELMs with smaller intensity. The likelihood of a postcursor ELM, and their number, increases with gas puffing rate, and these small postcursor events come to dominate numerically. Whereas ELMs with large D_α amplitude have a broad inter-ELM time interval distribution, the distribution of the postcursors is very sharply defined and is invariant between the three JET plasmas, see Fig.2. The inverse of this time interval defines a potentially important characteristic frequency of the ELMing process. The clear changes in ELMing displayed in Fig. 1, and for Pulse No's: 57867 to 57869, arise under comparatively small changes in gas puffing, see Fig.3; while there is a relatively large change between Pulse No's: 57865 and 57867. Other ELM interval dynamics are in principle possible for other gas fuelling rates, especially for fuelling rates between those of Pulse No's: 57865 and 57867.

CONCLUSIONS

We have exploited[7] the similarity of these six JET plasmas which have exceptionally long-duration (~5s) quasi-stationary ELMing processes. They appear to have only one control parameter, the gas puffing rate. These plasmas yield a sufficient number of ELMs and inter-ELM times, to enable us to apply the delay plot technique to characterize the dynamics, which is found to be low dimensional. ELM interval analysis of the kind presented here, if applied more widely, will shed light on transitions in confinement phenomenology in tokamak plasmas. Demonstrating and quantifying the effectiveness of ELM control and mitigation techniques will be assisted by characterizing the measured sequences of inter-ELM time intervals in this way.

ACKNOWLEDGEMENTS

This work was part-funded by the RCUK Energy Programme under grant EP/I501045 and the European Communities under the contract of Association between EURATOM and CCFE. The

views and opinions expressed herein do not necessarily reflect those of the European Commission. We acknowledge the UK EPSRC and the Chilean committee of science and technology, CONICYT, for support.

REFERENCES

[1]. A. Loarte et al., Plasma Physics and Controlled Fusion **45**, 1549 (2003)

[2]. K. Kamiya et al., Plasma Physics and Controlled Fusion **49**, S43 (2007)

[3]. R.J. Hawryluk et al., Nuclear Fusion **49**, 065012 (2009)

[4]. A. Degeling, Y. Martin, P.E. Bak, J.B. Lister, and X. Llobet, Plasma Physics and Controlled Fusion **43**, 1671 (2001)

[5]. J. Greenhough, S.C. Chapman, R.O. Dendy, and D.J. Ward, Plasma Physics and Controlled Fusion **45**, 747 (2003)

[6]. A.J. Webster and R.O. Dendy, Physical Review Letters **110**, 155004 (2013)

[7]. F.A. Calderon, R.O. Dendy, S.C. Chapman, A J Webster, B Alper et al., Physics of Plasmas **20**, 042306 (2013)

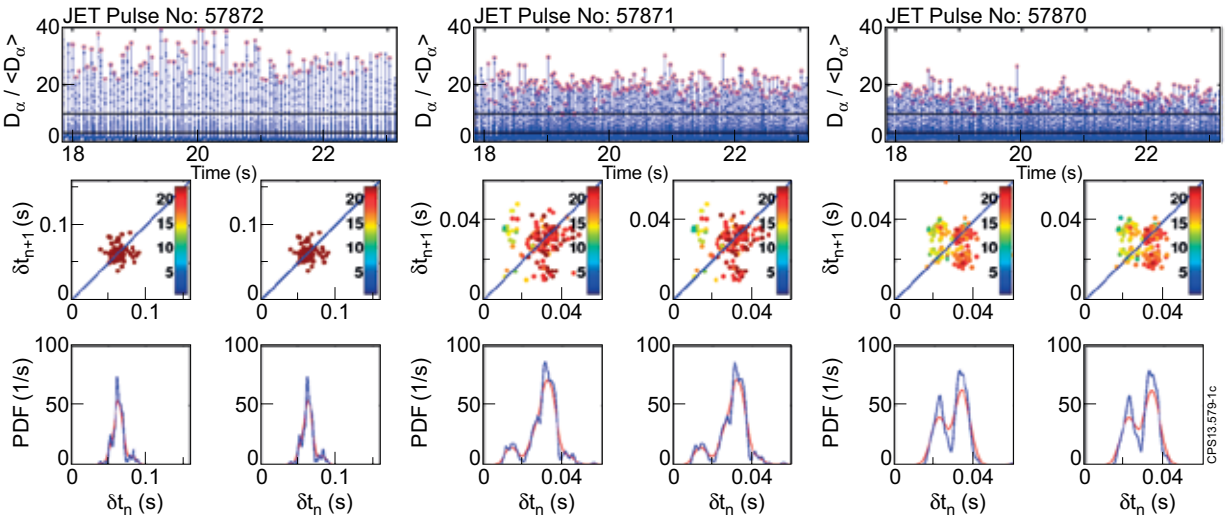

Figure 1. ELM characteristics of three similar JET Pulse No's: 57872, 57871, 57870 at lower gas puffing rates: (top of each panel) the time trace of D_α signal intensity, displaying the two amplitude thresholds used for the centre and bottom plots; (centre of each panel) delay plots for ELMs, with amplitude colour coded above the higher (lower) threshold on the left (right); (bottom of each panel) probability density functions for the distributions of measured δt_n for the ELM time series, using the same amplitude thresholds as for the delay plots; the red and blue curves represent different binning of the same data. The three plasmas are ordered, from the left, in increasing magnitude of gas puffing, see Fig.3. Reproduced from Ref. [7].

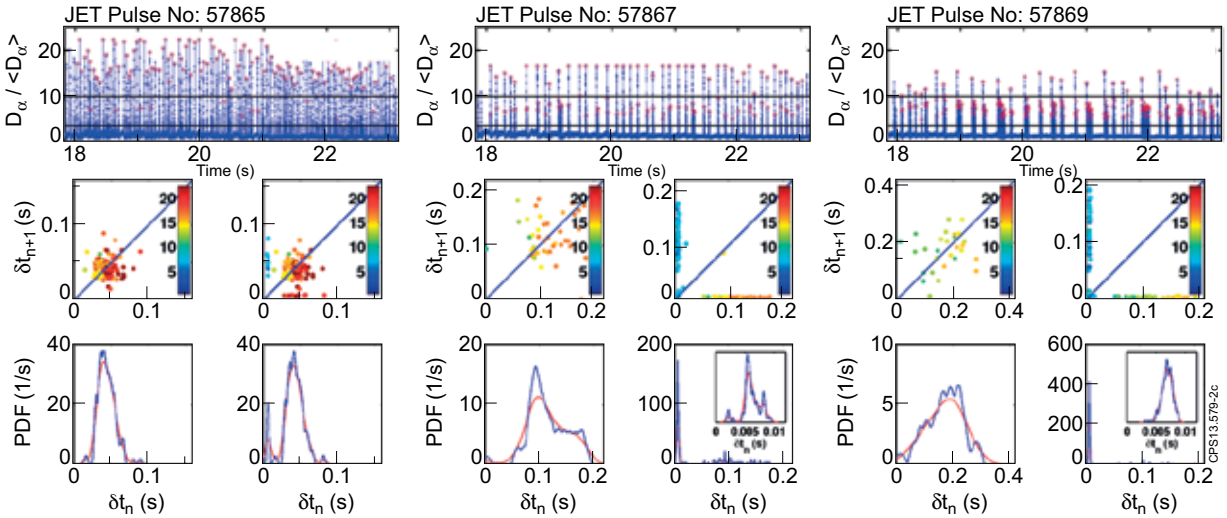

Figure 2: As Fig.1, for three similar JET Pulse No's: 57865, 57867, 57869 at higher gas puffing rates. The three plasmas are ordered, from the left, in terms of increasing magnitude of gas puffing, see Fig.3. The bottom panels from JET Pulse No's: 57867 and 57869 also include an inset panel displaying the sharp peak in the PDF. The population in this sharp peak increases with the gas puffing rate. Reproduced from Ref. [7].

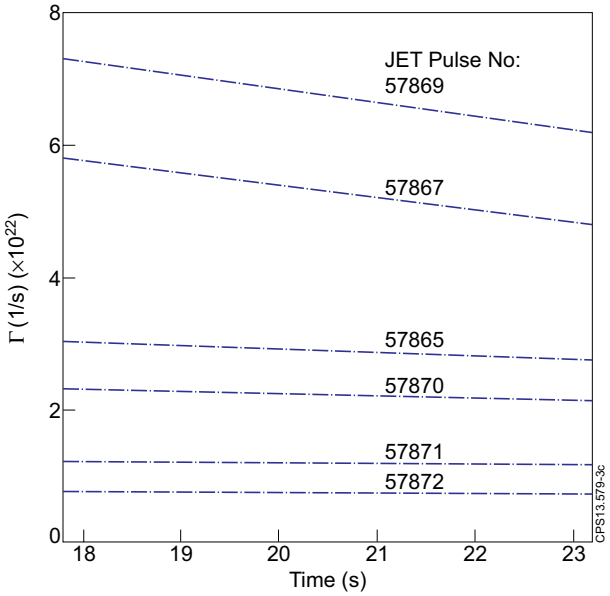

Figure 3: Time trace of gas puffing rate, Γ, in particles per second, which is the primary external control parameter for these six otherwise similar JET plasmas. Reproduced from Ref. [7].